First publ. in: Optics Express 18 (2010), 9, pp. 9251-9257

Impulsive terahertz radiation with high electric fields from an amplifier-driven large-area photoconductive antenna

M. Beck[1], H. Schäfer[1], G. Klatt[1], J. Demsar[1], S. Winnerl[2], M. Helm[2] and T. Dekorsy[1]

[1]*Department of Physics and Center for Applied Photonics, University of Konstanz, D-78457 Konstanz, Germany*

[2]*Forschungszentrum Rossendorf, Institute of Ion Beam Physics and Materials Research, POB 51 01 19, D-01314 Dresden, Germany*

Matthias.Beck@uni-konstanz.de

Abstract: We report on the generation of impulsive terahertz (THz) radiation with 36 kV/cm vacuum electric field (1.5 mW average thermal power) at 250 kHz repetition rate and a high NIR-to-THz conversion efficiency of 2×10^{-3}. This is achieved by photoexciting biased large-area photoconductive emitter with NIR fs pulses of μJ pulse energy. We demonstrate focussing of the THz beam by tailoring the pulse front of the exciting laser beam without any focussing element for the THz beam. A high dynamic range of 10^4 signal-to-noise is obtained with an amplifier based system.

OCIS codes: (320.7130) Ultrafast processes in condensed matter, including semiconductors; (300.6495) Spectroscopy, terahertz

References and links

1. B. Ferguson, and X.-C. Zhang, "Materials for terahertz science and technology, Nat. Mater. **1**," 26-33 (2002).
2. G. Klatt, F. Hilser, W. Quiao, M. Beck, R. Gebs, A. Bartels, K. Huska, U. Lemmer, G. Bastian, M. B. Johnston, M. Fischer, J. Faist, and T. Dekorsy, "Terahertz emission from lateral photo-Dember currents", Opt. Express **18**(5), 4939-4947 (2010).
3. A. Sell, A. Leitenstorfer, and R. Huber, "Phase-locked generation and field-resolved detection of widely tunable terahertz pulses with amplitudes exceeding 100 MV/cm," Opt. Lett. **33**, 2767-2769 (2008).
4. T. Bartel, P. Gaal, K. Reimann, M. Woerner, and T. Elsaesser, "Generation of single-cycle THz transients with high electric-field amplitudes," Opt. Lett. **30**, 2805-2807 (2005).
5. K.-L. Yeh, M. C. Hoffmann, J. Hebling and K. A. Nelson, "Generation of 10 μJ ultrashort terahertz pulses by optical rectification," Appl. Phys. Lett. **90**, 171121-1 (2007).
6. K.-L. Yeh, J. Hebling, M. C. Hoffmann and K. A. Nelson, "Generation of high average power 1 kHz shaped THz pulses via optical rectification," Opt. Commun. **281**, 3567-3570 (2008).
7. J. Hebling, K.-L. Yeh, M. C. Hoffmann, B. Bartal and K. A. Nelson, "Generation of high-power terahertz pulses by tilted-pulse-front excitation and their application possibilities," J. Opt. Soc. Am. B **25**, B6-B19 (2008).
8. M. Jewariya, M. Nagai and K. Tanaka, "Enhancement of terahertz wave generation by cascaded $\chi^{(2)}$ processes in $LiNbO_3$," J. Opt. Soc. Am. B. **26**, A101-A106 (2009).
9. G. Zhao, R. N. Schouten, N. van der Valk, W. Th. Wenckebach, and P. C. M. Planken, "Design and performance of a THz emission and detection setup based on a semi-insulating GaAs emitter", Rev. Sci. Instrum. **73**, 1715-1719 (2002).
10. A. Dreyhaupt, S. Winnerl, M. Helm, and T. Dekorsy, "Optimum excitation conditions for the generation of high-electric-field terahertz radiation from an oscillator-driven photoconductive device," Opt. Lett. **31**, 1546-1548 (2006).

#125169 - $15.00 USD Received 8 Mar 2010; revised 8 Apr 2010; accepted 8 Apr 2010; published 19 Apr 2010

11. J. Shan, and T. F. Heinz, *Terahertz radiation from semiconductors* (Springer Verlag, 2004).
12. G. Matthäus, S. Nolte, Rico Hohmuth, M. Voitsch, W. Richter, B. Pradarutti, S. Riehemann, G. Notni, and A. Tünnermann, "Microlens coupled interdigital photoconductive switch," Appl. Phys. Lett. **93**, 091110-1 (2008).
13. T. Hattori, K. Egawa, S.-I. Ookuma, and T. Itatani, "Intense terahertz pulses from large-aperture antenna with interdigitated electrodes," Jpn. J. Appl. Phys. **45**, L422-L424 (2006).
14. A. Dreyhaupt, S. Winnerl, T. Dekorsy, and M. Helm, "High-intensity terahertz radiation from a microstructured large-area photoconductor," Appl. Phys. Lett. **86**, 121114-1 (2005).
15. B. B. Hu, J. T. Darrow, X.-C. Zhang, D. H. Auston, and P. R. Smith, "Optically steerable photoconducting antennas," Appl. Phys. Lett. **56**, 886-888 (1990).
16. A. Leitenstorfer, S. Hunsche, J. Shah, M. C. Nuss, and W. H. Knox, "Femtosecond high-field transport in compound semiconductors," Phys. Rev. B **61**, 16642-16652 (2000).
17. G. Cho, W. Kütt, and H. Kurz, "Subpicosecond time-resolved coherent-phonon oscillations in GaAs," Phys. Rev. Lett. **65**, 764-766 (1990).
18. A. Leitenstorfer, S. Hunsche, J. Shah, M. C. Nuss and W. H. Knox, "Detectors and sources for ultrabroadband electro-optic sampling: Experiment and theory," Appl. Phys. Lett. **74**, 1516-1518 (1999).
19. A. E. Iverson, G. M. Wysin, D. L. Smith, and A. Redondo, "Overshoot in the response of a photoconductor excited by subpicosecond pulses," Appl. Phys. Lett. **52**, 2148-2150 (1988).
20. J. T. Darrow, X.-C. Zhang, D. H. Auston, and J. D. Morse, "Saturation properties of large-aperture photoconductive antennas," IEEE J. Quantum Electron. **28**, 1607-1616 (1992).
21. Z. Piao, M. Tani, and Kiyomi Sakai, "Carrier dynamics and terahertz radiation in photoconductive antennas," Jpn. J. Appl. Phys. **39**, 96-100 (2000).
22. D. S. Kim, and D. S. Citrin, "Coulomb and radiation screening in photoconductive terahertz sources," Appl. Phys. Lett. **88**, 161117-1 (2006).
23. J.-H. Son, T. B. Norris, and J. F. Whitaker, "Terahertz electromagnetic pulses as probes for transient velocity overshoot in GaAs and Si," J. Opt. Soc. Am. B **11**, 2519-2527 (1994).
24. M. B. Johnston, D. M. Whittaker, A. Corchia, A. G. Davies, and E. H. Linfield, "Simulation of terahertz generation at semiconductor surfaces," Phys. Rev. B **65**, 165301-1 (2002).
25. J. K. Luo, H. Thomas, D. V. Morgan, D. Westwood, and R. H. Williams, "The electrical breakdown properties of GaAs layers grown by molecular beam epitaxy at low temperature," Semicond. Sci. Technol. **9**, 2199-2204 (1994).

1. Introduction

Today, generation of radiation in the terahertz frequency range is a well established technique and can be used for many applications both in science and technology [1]. There exists a large variety of possible sources depending on the desired frequency range, the most important ones being acceleration of photoinduced carriers in semiconductors by external biasing or using the photo-Dember effect and nonlinear optical methods, such as optical rectification and difference-frequency mixing. While photoconductive methods have been used mostly for systems driven by a Ti:Sapphire oscillator, amplifier laser systems are usually used with THz sources based on nonlinear effects, owing to large material destruction thresholds and high conversion efficiencies. Another promising attempt in terms of frequency range and emission amplitude is using photo-Dember currents for THz emission, that already provides broadband THz pulses with a somewhat higher peak frequency compared to extrinsic biasing of photoconductors, as was already shown [2]. Nonlinear optical conversion already provides large electric fields in the MV/cm regime or less and with tunable center frequencies in the $10-100$ THz range [3, 4], whereas electric field strength and frequency range both depend strongly on the excitation pulse properties, namely pulse energy and pulse length. Typically, for electric field values of tens of kV/cm or higher one needs excitation pulse energies as high as hundreds μJ or above. In materials like $LiNbO_3$ a special excitation geometry, namely tilted-pulse-front excitation is additionally required [5, 6, 7, 8]. In this letter we report generation of high THz electric fields in the $0.2-4$ THz range up to 36 kV/cm in vacuum using a microstructured large-area photoconductor in combination with an amplifier laser system running at 250 kHz repetition rate. Due to the strong THz electric field a high dynamic range is achieved, which is comparable to the value of low-noise oscillator-driven systems [9]. Moreover we show that large-area PC antennas provide high conversion efficiencies even when excited at high fluences in the μJ/cm^2 regime. The

#125169 - $15.00 USD Received 8 Mar 2010; revised 8 Apr 2010; accepted 8 Apr 2010; published 19 Apr 2010

measured average thermal power of the THz radiation reaches a maximum of 1.5 mW when exciting the photoconductor with 800 mW of NIR power at 70 kV/cm static acceleration field. Thus a conversion efficiency of 2×10^{-3} is calculated, which is one order of magnitude higher than previous reports on PC antennas [10]. The measured electric fields are the highest reported so far in the 1 THz range, when exciting photoconductive antennas with μJ optical pulses.

Up to now, several attempts have been made to increase the electric field strength emitted by photoconductive switches. Several saturation effects present in semiconducting materials at high excitation densities prevent a linear scaling of THz emission with excitation fluence [11]. Matthäus *et al.* [12] used an interdigitated finger electrode structure similar to the one presented here but prepared on a low-temperature grown GaAs substrate. A Ti:Sa oscillator is used to excite an active area of 1×1 mm^2. Moreover they built a hexagonal lens array above the finger electrodes to control the illuminated area on the PC. In this case only every second electrode spacing is excited by the optical pulses. With this setup, higher optical power can be injected into the semiconductor than without the lens. Recently they reported generation of THz pulses with 280 μW average thermal power, however, NIR-to-THz conversion efficiency stays in the 10^{-4} regime. Another experiment was carried out by Hattori *et al.* [13] which used an amplified laser system at a repetition rate of 1 kHz to excite the photoconductor. For reduction of saturation effects they placed 7 equal microstructured devices beneath each other on a common GaAs wafer, thus effectively increasing the active area. However the achieved THz field did not overcome the values of conventional large-area PCs and equal scaling of the emitted THz field with size was not observed.

2. Setup Scheme

In this work we investigate THz emission from the acceleration of photoinduced carriers in GaAs at high excitation densities. For this purpose, a photoconductive antenna with a specific metal-semiconductor-metal (MSM) structure is used, whose detailed description can be found in [14]. The structure consists of interdigitated finger electrodes processed by optical lithography on a semi-insulating GaAs substrate. The electrodes width and spacing are 5 μm, respec-

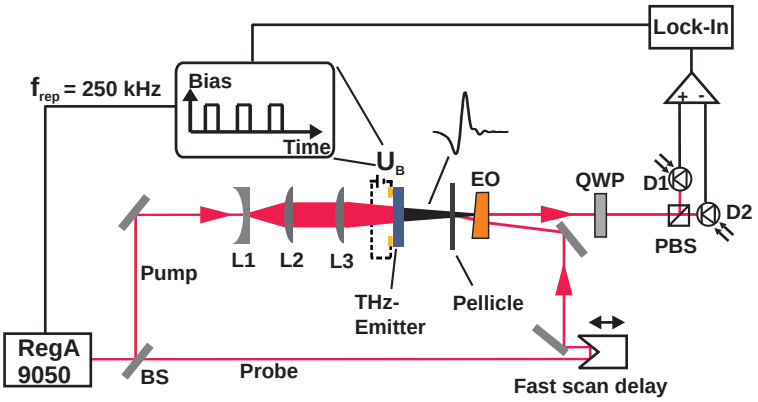

Fig. 1. Beam splitter plate (BS) divides optical pulse trains from the amplifier in pump and probe beam; Lenses (L1,L2) enlarge the pump spot and lense (L3) focus the beam; Emitter bias voltage U_B is modulated at laser repetition rate; Electro-optic crystal (EO), quarter-wave plate (QWP), beam splitter cube (PBS) and two photodiodes (D1,D2) are used to probe THz transients. Note that there is a THz focus at the position of the EO crystal without use of additional optics, i.e. parabolic mirrors.

#125169 - $15.00 USD Received 8 Mar 2010; revised 8 Apr 2010; accepted 8 Apr 2010; published 19 Apr 2010

tively. Every second electrode gap is covered with an additional metallization isolated from the electrodes. This leads to an unidirectional electric bias field over the whole excited area of the PC device, and thus constructive interference of adjacent active areas in the far-field. Because of the small electrode spacing, acceleration of free carriers at high electric fields close to the breakdown field of semi-insulating GaAs is achieved at bias voltages of some tens of volts. Additionally the structure can be scaled easily to a large active area of 1×1 cm^2. For the experiments, we used a commercial regenerative amplifier laser system (RegA 9050, Coherent Inc.), generating < 50 fs pulses at 800 nm center frequency and 250 kHz repetition rate with pulse energies up to 4 μJ. The basic concept of the setup is shown in Fig. 1. The optical pulse trains are divided into a pump and a probe branch, whereas the pump beam waist is enlarged to several millimeters using a telescope (L1,L2) before it is being focused by a third lens (L3) with a short focal length of f $= 35$ mm. The PC antenna is placed at normal incidence at a distance smaller than the focal lense to prevent destruction of the device by keeping the illuminated area large. The generated THz radiation conserves the NIR phase front information [15]. Hence a THz focus is observed at a distance of approximately f $= 35$ mm after L3. In this configuration no additional optics are required for collimation and focusing of the THz radiation. A conventional electro-optic detection scheme is used for probing the far-infrared transients in a 350 μm thick ZnTe crystal in combination with conventional balanced difference detection [16]. Collinear propagation for THz and optical probe beam in the EO crystal is achieved by placing a 2 μm thick pellicle beam splitter between antenna and the EO crystal. The probe beam is delayed periodically relative to the pump (THz) beam by a retroreflector mounted on an electro-mechanical shaker, that runs at 28 Hz [17]. Hence one complete time trace of 20 ps is acquired within 35 ms of measurement time. Chopping of the THz signal at 62 kHz is performed electronically by modulating the emitter bias at a fraction of the laser repetition rate for low noise lock-in detection. Maximum values for the relative intensity change $\Delta I/I$ (EO signal) are on the order of 10^{-1}. Within 20 s of measurement time the noise floor drops down to a few 10^{-5}, hence a high dynamic range of 10^4 in electric field amplitude is achieved. Owing to the large average thermal power of the THz radiation, the beam waist can easily be mapped using a standard knife-edge method and a high sensitivity low power thermopile detector. We determined the beam waist radius (1/e^2 of intensity) at the focus to be 1.1 mm.

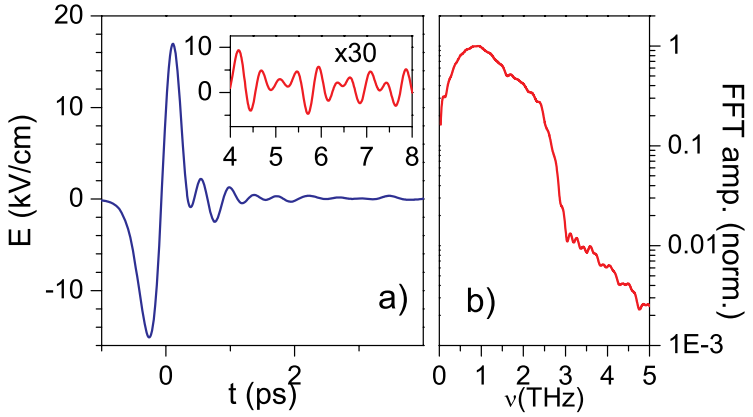

Fig. 2. The time trace shows the maximum THz electric field detected in the EO crystal equals 17 kV/cm. The magnified part shows oscillations occurring due to absorption and reemission of THz radiation by water vapor. Because of the high SNR the magnified oscillations appear without visible noise. Next to the time trace window the corresponding (normalized) spectral amplitude is shown.

#125169 - $15.00 USD Received 8 Mar 2010; revised 8 Apr 2010; accepted 8 Apr 2010; published 19 Apr 2010

3. Results

The experimental data presented in this work were collected with two photoconductive antennae described earlier, however the two devices show different dark resistances 100 Ω and 0.5 MΩ respectively. The overall maximum value for the THz electric field was achieved with the device having the higher dark resistivity and therefore lower dark current. The corresponding transient shown in Fig. 2 peaks at a value of 17 kV/cm. This value corresponds to the THz electric field amplitude detected in the ZnTe electro-optical crystal. To calculate the vacuum electric field from this value, one has to correct for Fresnel reflection losses at the crystal entrance surface and for the frequency dependent response of the ZnTe electro optic crystal [18]. In the investigated frequency range almost no frequency distortion is observed when comparing the measured THz pulse to the calibrated THz waveform in vacuum. After correcting for Fresnel losses with a constant refractive index for ZnTe of 3.17 [7], one obtains a vacuum electric field of 36 kV/cm. This value is in agreement when compared to the value of the THz vacuum electric field calculated from the average thermal power which we measured. The inset of Fig. 2 shows the spectral amplitude of the measured THz pulse that peaks at 1 THz. Spectral components are visible up to 3 THz where the signal drops to 20 dB. With this device the highest applied bias voltage was kept below 25 V to prevent degradation of the device. The data collected with the device having the smaller dark resistance and therefore higher dark current is shown in Figs. 3 and 4.

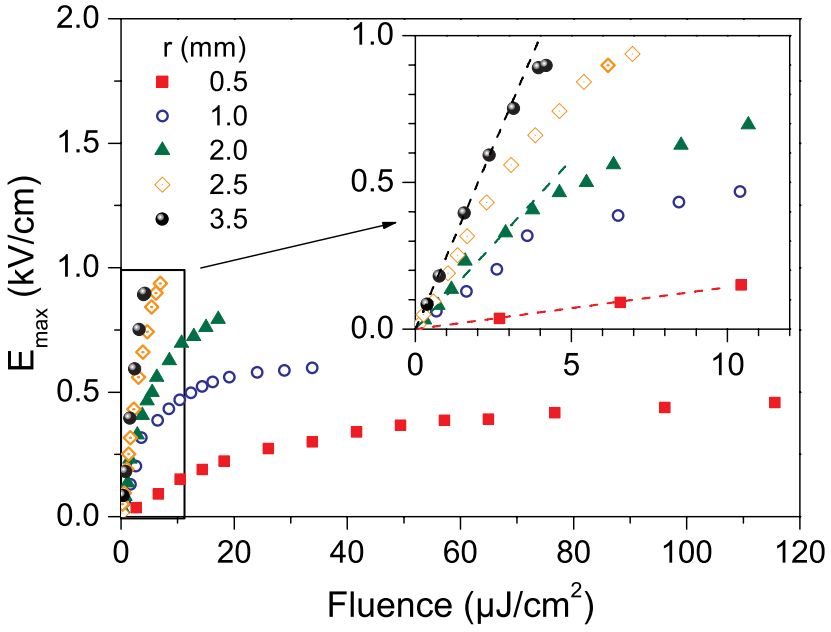

Fig. 3. Maximum THz electric field as a function of excitation fluence and excitation spot size radius ($1/e^2$) on the PC. The dashed lines in the inset correspond to the expected linear dependence in the vicinity of saturation effects. All measurement points were acquired at an acceleration field of 20 kV/cm to reduce additional saturation effects present at high bias electric fields [19].

To find optimal excitation parameters, we first investigated the dependence of the emitted THz electric field amplitude on the optical excitation power at several illumination spot sizes on the PC. The setup configuration shown in Fig. 1 allows variation of optical excitation spot size

#125169 - $15.00 USD Received 8 Mar 2010; revised 8 Apr 2010; accepted 8 Apr 2010; published 19 Apr 2010

by simply moving the antenna in the direction of the beam. Figure 3 shows the corresponding saturation curves, where the excitation spot size was varied from 0.5 mm to 3.5 mm beam waist radius ($1/e^2$). As follows from the magnification in the inset in Fig. 3, a linear dependence can be observed at low excitation densities for all spot sizes. The dashed lines represent the slopes at three different spot sizes. From theory a linear increase of THz amplitude at low excitation power is expected [20]. At high excitation densities, several effects occur in the semiconductor device that lead to a deviation from linearity. One of the reasons is the well-known screening of the bias acceleration field due to the separation of optically induced free carriers and the resulting build up of a strong polarization [11, 21]. Additionally to this Coulomb-screening, the bias field is reduced by the generated THz electric field itself, so called near-field screening. The latter becomes more important as the excitation spot size increases [22]. Both effects scale with the free carrier density, thus reduction of screening effects can be achieved by simply enlarging the excitation area on the PC. Simultaneously, THz emission is increased due to a larger excitation area on the PC. This effect can be estimated from the slope of the fit curves in the inset. Changing the excitation spot size from 0.5 mm to 3.5 mm, the output radiation at low excitation densities can be increased by about one order of magnitude. Efficient scaling of THz emission is possible as long as the excitation power and spot size can be increased simultaneously. Here, limitations are given by the PC active area of 1×1 cm^2 and maximum laser output power of 1 W. During the measurements shown in Fig. 3 the bias electric field was kept at of 20 kV/cm. This value is higher than the Gunn-field in GaAs (5.3 kV/cm) [16]. Strong saturation of THz emission by the Fröhlich-type interaction is expected at much higher acceleration fields [23].

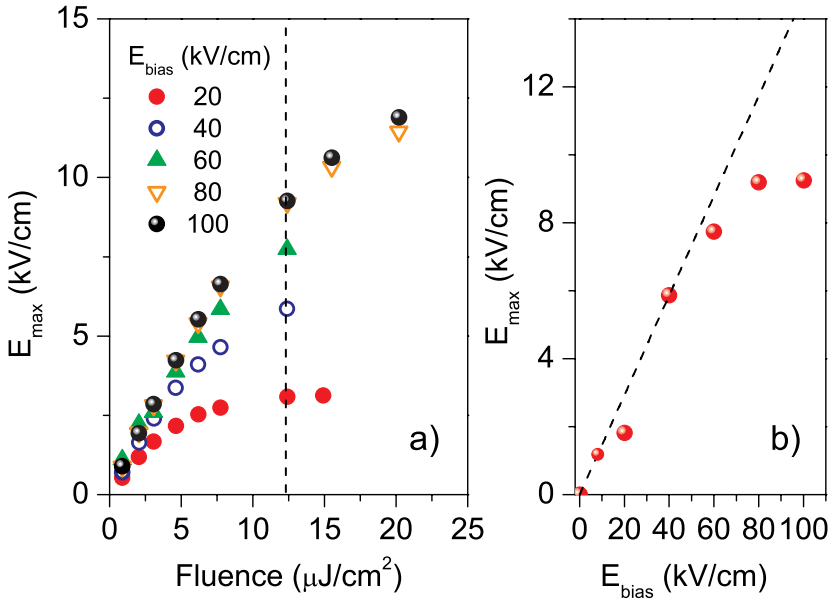

Fig. 4. Maximum THz electric field as a function of excitation fluence on the PC for different acceleration fields. The range where THz amplitude scales linearly with fluence is significantly extended at higher bias fields. The graph to the right shows a vertical cut of the curves in the left graph at a fixed excitation fluence of 12.4 μJ/cm^2. A linear dependence of THz amplitude is observed up to acceleration fields of 40 kV/cm. At higher bias fields saturation of THz emission occurs due to ultra-fast transfer of free carriers into the side-valleys of GaAs [19].

#125169 - $15.00 USD Received 8 Mar 2010; revised 8 Apr 2010; accepted 8 Apr 2010; published 19 Apr 2010

We also investigated the effects of the acceleration field on THz emission as a function of the excitation fluence. It can be seen that the range over which the THz amplitude scales linearly with fluence is extended as the bias field increases. This is an indication for the fact, that near-field screening effects become less significant at higher acceleration fields, since the magnitude of the near-field is reduced relatively to the magnitude of the external bias field. Also the slope of the curves increase as function of the acceleration field. The inset of Fig. 4 shows a "vertical cut" of the curves at a fixed fluence of 12.4 μJ/cm^2. A linear scaling of THz amplitude with the bias electric field can be seen up to acceleration fields around 40 kV/cm. This behavior is in agreement with theoretical models for the photocurrent in the PC [20] and also with Monte-Carlo simulations [24]. In contrast, at higher electric fields additional saturation mechanisms occur leading to a reduction of the THz emission. Mainly this reduction can be attributed to ultra-fast scattering of free carriers from the Γ-Valley into the side-valleys (namely L- and X-valley) of the conduction band of GaAs via the deformation potential. Carriers in these side-valleys exhibit a strongly reduced mobility [19], which effectively decreases the transient photocurrent in the PC. Maximum values of the acceleration field is limited by the breakdown field of semi-insulating GaAs. This could be enhanced by using low-temperature grown GaAs as substrate [25]. Moreover the time constant for intervalley scattering in the high-field transport regime in GaAs is on the order of 20 fs [16], as also may be estimated from a simple ballistic transport model [23]. These high frequency dynamics cannot be detected in the present setup due to the ZnTe crystal thickness of 350 μm and the probing pulse length of 60 fs, so additional loss of amplitude is expected in the high-field transport regime due to the limited detection bandwidth.

4. Conclusion

In conclusion, we presented a way to generate impulsive THz radiation by driving a photoconductive antenna with amplified laser pulses at 250 kHz. By the use of a specific MSM structure on the PC and a large active area of about 1×1 mm^2 saturation effects such as bias screening may effectively be reduced, therefore allowing the use of high optical energy for excitation. In our case optimum conditions have been achieved with an excitation density of 20 μJ/cm^2 and 70 kV/cm bias acceleration field. With these conditions THz electric fields around 17 kV/cm could be measured in the ZnTe crystal, corresponding to a vacuum electric field of 36 kV/cm. We determined the average thermal power to be 1.5 mW, which is one order of magnitude higher compared to the values achieved with other photoconductors [13] or using an oscillator [10]. This value corresponds to a high conversion efficiency of 2 x 10^{-3}.

5. Acknowledgements

This research is supported by the Landesstiftung Baden-Württemberg, the German Israeli DIP project and the Sofja Kovalevskaja Award of the Alexander von Humboldt Foundation. Financial support of the Center for Applied Photonics (CAP) is gratefully acknowledged.

#125169 - $15.00 USD Received 8 Mar 2010; revised 8 Apr 2010; accepted 8 Apr 2010; published 19 Apr 2010